

# Multiple-objective microscopy with three-dimensional resolution near 100 nm and a long working distance

O. Haeberlé, C. Xu, A. Dieterlen, and S. Jacquey

Groupe Lab. El-Laboratoire Modélisation Intelligence Processus Systèmes, Université de Haute-Alsace, Institut Universitaire de Technologie de Mulhouse, 61 Rue A. Camus, F-68093 Mulhouse Cedex, France

Received June 1, 2001

The resolution of microscopes is limited by the sizes of their point-spread functions. The invention of confocal, theta, and 4Pi microscopes has permitted the classic Abbe limit to be exceeded. We propose the use of a combination of 4Pi and theta microscopy to decrease resolution by using four illumination objectives and two detection objectives. Using middle numerical aperture, long-working-distance objectives yielded a resolution near 100 nm in the three dimensions, which opens the possibility of exploring large volumes with a high resolution. © 2001 Optical Society of America

OCIS codes: 180.2520, 180.6900, 110.0180, 110.6880.

Fluorescence microscopy is a key tool with which to study three-dimensional structures of living cells and tissues.<sup>1-3</sup> The invention of confocal, theta, and 4Pi microscopes has permitted the conventional resolution limit to be overcome.<sup>4-6</sup> With these instruments, an increase in resolution is obtained by optical means; thus the illumination and detection processes have been improved. Stimulated-emission depletion microscopy, a recently proposed technique, promises to push the resolution limit even further.<sup>7</sup> In this approach, one uses quantum effects to prevent the occurrence of fluorescence in places where it is not desired, effectively reducing the actual size of the point-spread function (PSF). A resolution of the order of 100 nm in three dimensions has been obtained.

We propose to combine and extend 4Pi and theta microscopy in a multiple objective microscopy (MOM) configuration by using four illumination and two detection objectives, and we show that the theoretical resolution achievable in this configuration is similar to that of stimulated-emission depletion microscopy.

Here we consider, for simplicity, water-immersion objectives used without coverslips. In this case, the Richard-Wolf model of diffraction describes PSF formation well.<sup>8</sup> Also, the configuration that we consider does not allow coverslips to be used.<sup>6</sup>

The electric field at point  $x, y, z$  (see Fig. 1) in the focal region of a single lens can be written as

$$\begin{aligned} E_x(x, y, z) &= -i(I_0 + I_2 \cos 2\phi), \\ E_y(x, y, z) &= -i(I_2 \sin 2\phi), \\ E_z(x, y, z) &= -2I_1 \cos \phi, \end{aligned} \quad (1)$$

where for a system illuminated by a plane-polarized wave one has (neglecting a constant factor)

$$\begin{aligned} I_0 &= \int_0^a a(\theta) \sin \theta (1 + \cos \theta) J_0(kr \sin \theta) \exp(ikz \cos \theta) d\theta, \\ I_1 &= \int_0^a a(\theta) \sin^2 \theta J_1(kr \sin \theta) \exp(ikz \cos \theta) d\theta, \\ I_2 &= \int_0^a a(\theta) \sin \theta (1 - \cos \theta) J_2(kr \sin \theta) \exp(ikz \cos \theta) d\theta. \end{aligned} \quad (2)$$

In Eqs. (2),  $a(\theta)$  is the apodization function, which for an aberration-free system that obeys the sine condition is given by  $a(\theta) = \cos^{1/2} \theta$ , where  $r$  is the radial distance from the origin in cylindrical coordinates and  $\phi$  is the angle between the direction of observation of point P and the incident wave's polarization axis. We consider a linearly polarized wave with the  $E$  vector lying along the  $x$  axis (see Fig. 1).

The intensity PSF can then be computed as

$$\begin{aligned} \text{PSF}_{\text{ill}}(x, y, z) &= |E(x, y, z)|^2 = |I_0|^2 \\ &+ 4|I_1|^2 \cos^2 \phi + |I_2|^2 + 2 \text{Re}(I_0 I_2^*) \cos 2\phi. \end{aligned} \quad (3)$$

Equation (3) corresponds to computation of the intensity detection PSF of an optical microscope with wide-field illumination. The illumination can be linearly, circularly, or randomly polarized. When it is assumed that the fluorescence mechanism implies only randomly polarized emission, the  $\phi$  dependence vanishes, and the intensity detection PSF is given by

$$\text{PSF}_{\text{det}}(x, y, z) = |I_0|^2 + 2|I_1|^2 + |I_2|^2. \quad (4)$$

Descriptions of the image formation process for other cases of fluorescence emission can be found in Refs. 9 and 10. For a 1.4-N.A. objective, Eq. (4) leads to a lateral resolution of 200 nm and an axial resolution of 450 nm at a wavelength of 450 nm. The intensity PSF of a confocal microscope is to a first approximation the square of that of a classical microscope. (For a more detailed theory of

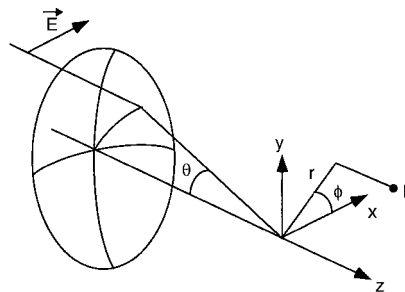


Fig. 1. Light linearly polarized along the  $x$  axis and focused by a lens in a single medium. Cylindrical coordinates are used.

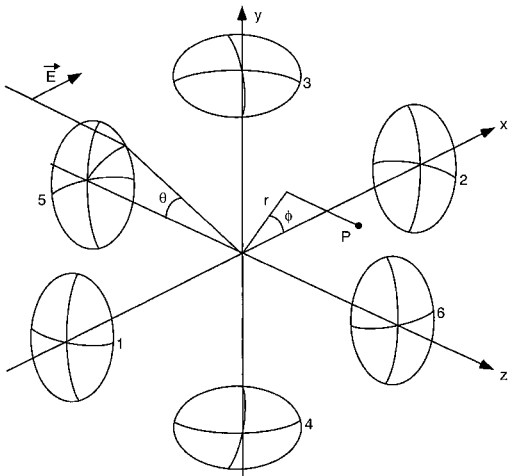


Fig. 2. Multiple-objective configuration considered in this Letter. Illumination comes from coherent addition of the focal fields of objectives 1–4. Objectives 5 and 6 are used in the 4Pi detection mode.

high-N.A. confocal microscopy, the interested reader is referred to Refs. 9 and 10 and references therein.) This approximate formula leads to an estimation of the resolution for the confocal PSF with the same objective of dimensions 130 nm laterally and of 320 nm longitudinally. A 4Pi microscope uses two illumination objectives, adding their illumination fields coherently to detect the emission coherently (4Pi type C).<sup>5</sup> With the same parameters, the longitudinal resolution is dramatically improved to 70 nm; however, the gain in lateral resolution is less, with a FWHM of 120 nm. The principle of theta microscopy is to multiply spatially differently arranged illumination and detection PSFs to obtain a narrower global PSF.<sup>6</sup> But the necessary orthogonal arrangement leads to the use of low- or middle-N.A. objectives. So, even if the longitudinal resolution is better than that of a confocal microscope with a high aperture, the loss in lateral resolution is such that the global PSF is much larger.<sup>11</sup> Low-N.A. objectives, however, can work at longer distances in the millimeter range, and therefore large samples can be studied.<sup>6,11</sup>

In an attempt to combine the advantage of 4Pi microscopy with high-N.A. objectives (high resolution) and of theta microscopy (long working distance), we have studied other multiple-objective configurations. Figure 2 shows the configuration that we found gives the best results in terms of resolution. Four objectives along the  $x$  and  $y$  axes are used for interferometric illumination at 400 nm; the two objectives along the  $z$  axis are used for detection at 450 nm [corresponding to excitation and emission of Cascade Blue dye (Molecular Probes)]. This configuration can therefore be considered a modified 4Pi microscope that uses an illumination field that results from four interfering illumination beams instead of an illumination beam from one objective (4Pi type B microscopy) or two objectives (4Pi type C microscopy).

To compute the intensity illumination PSF, one has now to add the contributions of four objectives:

$$\text{PSF}_{\text{ill}}^{4\text{obj}}(x, y, z) = |E_x(x, y, z) + E_x'(x, y, z) + E_y(x, y, z) + E_y'(x, y, z)|^2. \quad (5)$$

One can easily compute the four electromagnetic fields from Eqs. (1) by applying the corresponding rotation. For random polarization illumination the angular dependences disappear and Eq. (5) reduces to

$$\begin{aligned} \text{PSF}_{\text{ill}}^{4\text{obj}}(x, y, z) = & \text{Re}(I_0')^2 + 2 \text{Re}(I_1')^2 + \text{Re}(I_2')^2 \\ & + \text{Re}(I_0'')^2 + 2 \text{Re}(I_1'')^2 + \text{Re}(I_2'')^2 + 2 \text{Re}(I_0')\text{Re}(I_0''). \end{aligned} \quad (6)$$

For a 4Pi setup, the intensity detection PSF is<sup>5</sup>

$$\text{PSF}_{\text{det}}^{2\text{obj}}(x, y, z) = \text{Re}(I_0)^2 + 2 \text{Re}(I_1)^2 + \text{Re}(I_2)^2, \quad (7)$$

$$I_n = I_n(x, y, z),$$

$$I_n' = I_n(y, z, -x),$$

$$I_n'' = I_n(y, z, x) \quad n = 1, 2, 3. \quad (8)$$

Figure 3 shows the illumination  $\text{PSF}_{\text{ill}}^{4\text{obj}}$ , the detection  $\text{PSF}_{\text{det}}^{2\text{obj}}$ , and the resultant  $\text{PSF}^{6\text{obj}}$ , which is the product of the other two. Illumination is performed at a wavelength of 400 nm; detection, at 450 nm with water-immersion objectives whose N.A. is 0.8. The resolution is 108 nm laterally and 89 nm axially. The sidelobes that are visible along the  $z$  axis can be removed by point filtering.<sup>11</sup> This result is interesting because middle-N.A. objectives are used. Thus one can see that high resolution is not restricted to high-N.A. objectives. Furthermore, as these objectives may have working distances in the millimeter range, MOM opens the possibility of exploring large volumes with a high resolution.

In Fig. 4 various setups are compared. Figure 4(a) shows the intensity PSF of the long-working-distance, water-immersion objective with a N.A. of 0.8 considered in this Letter. Figures 4(b) and 4(c) show the intensity PSFs for a 4Pi type C and a theta microscope, respectively, that use the same objectives. The 4Pi microscope exhibits a good longitudinal resolution, but the image obtained is difficult to interpret, as many interference fringes exist.<sup>12</sup> The theta microscope has a nearly isotropic resolution, but it is lower than one can obtain from a 4Pi microscope with large-N.A. objectives.<sup>11</sup> Figure 4(d) clearly shows the gain in resolution that one can expect with MOM compared with that of these other long-working-distance microscopes. The N.A. cannot be arbitrarily decreased, as illustrated by Fig. 4(e), which shows the intensity PSF for our setup with N.A. = 0.4 objectives. Whereas the resolution is not affected (as the central spot results from an interference process), the interference pattern is of much greater complexity, exhibiting several secondary maxima, and the resultant image would be contaminated by several parasitic ghosts; this would limit the possibilities of image restoration<sup>12</sup> [Figs. 4(a)–4(d) have been computed for Cascade Blue].

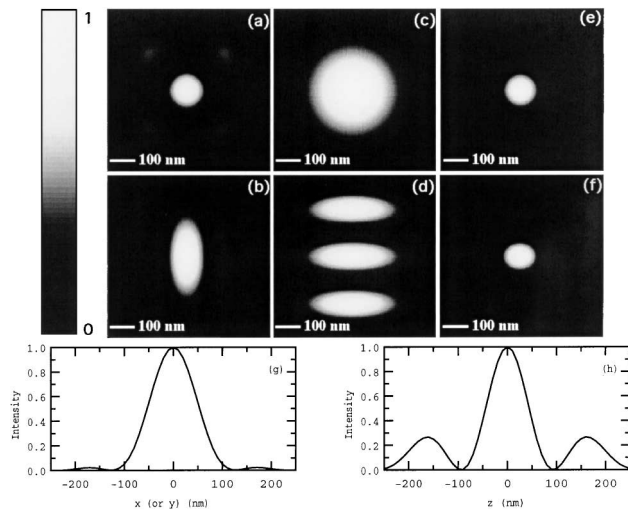


Fig. 3. Computed intensity PSF of a MOM: (a) illumination PSF in the  $(x, y, z = 0)$  plane, (b) illumination PSF in the  $(x, y = 0, z)$  plane, (c) detection PSF in the  $(x, y, z = 0)$  plane, (d) detection PSF in the  $(x, y = 0, z)$  plane (central part only), (e) final intensity PSF in the  $(x, y, z = 0)$  plane, (f) final intensity PSF in the  $(x, y = 0, z)$  plane, (g) lateral intensity distribution, (h)  $z$ -axis intensity distribution. The lateral resolution is 108 nm, and the longitudinal resolution is 89 nm. Illumination wavelength, 400 nm; detection wavelength, 450 nm (Cascade Blue from Molecular Probes); N.A. of water-immersion objectives, 0.8.

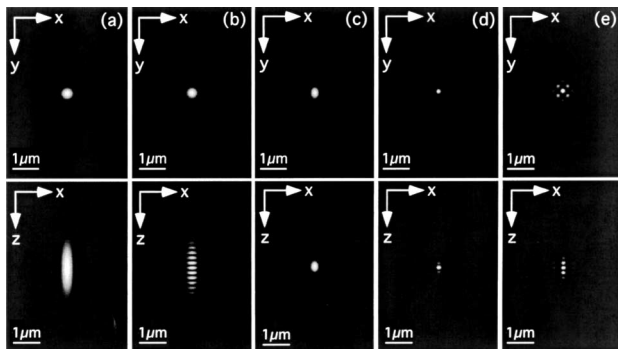


Fig. 4. Computed intensity PSFs for (a) single-objective, (b) 4Pi type C, (c) theta, and (d) MOM microscopes with N.A. = 0.8 water-immersion objective (same conditions as for Fig. 3). (e) Intensity PSF of a MOM with N.A. = 0.4 objective. The resultant interference pattern is more complex and exhibits several secondary maxima.

It is probably complex to set up MOM. It is, however, worth noting that the complexity of the illumination setup is reduced by the fact that it is separate from the detection setup, unlike in 4Pi type C microscopy. As a consequence, the optical paths do not have to be exactly the same, because of the long coherence length of the lasers. For the detection, the optical paths still have to be identical within the typical coherence length of fluorescence, namely, within  $\sim 20 \mu\text{m}$ .<sup>11</sup> The detection difficulty is therefore the same as for 4Pi type B and type C microscopy.

The objectives to be used must have long working distances to be placed at  $90^\circ$  while simultaneously avoiding contact with one another. We found the Olympus Universal Plan Fluorite  $40\times$  water-immersion,

N.A. = 0.8 objective with a working distance of 3.3 mm to be well suited for our purposes, after a small modification of the objective's enclosure.<sup>13</sup>

The use of a cubic waterproof enclosure with the six objectives passing through the six faces would ensure that the specimen was immersed in water and that this water could not leak out of the volume defined by the six objectives. The specimen itself would have to be manipulated with microtweezers<sup>14</sup> or be mounted upon a glass capillary fixed on a high-precision scan stage.<sup>15</sup> Small specimens could be handled with laser tweezers. However, for such samples a 4Pi microscope that uses high-N.A., short-working-distance objectives would probably be more useful, as it gives similar resolution with a less-complex setup.

In summary, we have shown that a combination of coherent four-objective illumination and coherent two-objective detection permits high resolution to be obtained near 100 nm in three dimensions by use of middle-N.A. objectives. Water-immersion objectives with a N.A. of 0.8 have long working distances in the millimeter range. MOM therefore has the unique feature of combining high resolution and large explorable volumes.

O. Haerberlé thanks H. Furukawa for valuable discussions on optical tweezers and microactuators. His e-mail address is o.haerberle@uha.fr.

## References

1. T. Wilson and C. J. R. Sheppard, *Theory and Practice of Scanning Optical Microscopy* (Academic, London, 1984).
2. D. A. Agard, Y. Hiraoka, P. Shaw, and J. W. Sedat, in *Fluorescence Microscopy in Three Dimensions*, D. L. Taylor and Y. Wang, eds., Vol. 30 of *Methods in Cell Biology* (Academic, San Diego, Calif., 1989), p. 353.
3. S. W. Hell, E. Lehtonen, and E. H. K. Stelzer, in *New Dimensions of Visualization in Biomedical Microscopies*, A. Kritte, ed. (Verlag Chemie, Weinheim, Germany, 1992), p. 145.
4. M. Minsky, *Scanning* **10**, 128 (1988).
5. S. W. Hell and E. H. K. Stelzer, *Opt. Commun.* **93**, 277 (1992).
6. E. H. K. Stelzer and S. Lindek, *Opt. Commun.* **111**, 536 (1994).
7. T. A. Klar, S. Jakobs, M. Dyba, A. Egner, and S. W. Hell, *Proc. Natl. Acad. Sci. USA* **97**, 8206 (2000).
8. B. Richards and E. Wolf, *Proc. R. Soc. London Ser. A* **253**, 349 (1959).
9. C. J. R. Sheppard and P. Török, *Bioimaging* **5**, 205 (1989).
10. P. D. Higdon, P. Török, and T. Wilson, *J. Microsc.* **193**, 127 (1999).
11. S. W. Hell, in *Nonlinear and Two-Photon Induced Fluorescence*, J. Lakowicz, ed., Vol. 5 of *Topics in Fluorescence Microscopy* (Plenum, New York, 1997), p. 361.
12. M. Nagorni and S. W. Hell, *J. Opt. Soc. Am. A* **18**, 49 (2001).
13. R. Clappier, Olympus France SA, 75 Rue d'Areueil 94533 Rungis, France (personal communication, 2001).
14. T. Tanikawa and T. Arai, *IEEE Trans. Robot. Autom.* **15**, 152 (1999).
15. J. Swoger, S. Lindek, T. Stefany, F.-M. Haar, and E. H. K. Stelzer, *Rev. Sci. Instrum.* **69**, 2956 (1998).